Drag Coefficient and Nusselt Number for Laminar Pulsating Flow in Porous Media

T.I. Mulcahey, M.G. Pathak, S.M. Ghiaasiaan

Cryo Lab, School of Mechanical Engineering
Georgia Institute of Technology, Atlanta, GA, USA 30332

ABSTRACT

In this paper transient (pulsating) flow in micro heat exchangers is numerically simulated. The objective is to examine the enhancement of heat transfer in heat exchangers by flow pulsation. Laminar 2-D pulsating flow of air through homogeneous arrays of ten rows of heated square rods is simulated for frequencies of 0-80 Hz. Cycle-average and maximum drag coefficients, and cycle-average Nusselt numbers are reported for each of the ten rods in the simulated array. A wake interference effect was observed which significantly amplifies the drag on the leading rods and reduces and instantaneously reverses the sign of the drag force on the rods located in the wake region. Cycle average drag is found to decrease with increasing Reynolds number and porosity, and is only a weak function of pulsation frequency. Peak drag was found to decrease with increasing Reynolds number and porosity, but linearly increase with increasing frequency. The cycle-average Nusselt number decreased with increasing porosity, but monotonically increased with both Reynolds number and frequency.

INTRODUCTION

The importance of cross-flow in tube and rod bundles is well recognized. Such flows are encountered in most heat exchangers. Although heat exchangers have been studied extensively, the vast majority of previous investigations [1-12] deal with steady flow because heat exchangers are normally designed to operate in steady state. Experimental measurement of the details of hydrodynamic and transport processes in the interstitial spaces in tube bundles is difficult because such measurements often cause significant flow disturbance. This is particularly true for miniature heat exchangers.

Unsteady and periodic flows in porous media are common in some of the key components of Stirling and pulse tube cryocoolers [13-16]. Pulsating flow in idealized porous media composed of periodically-configured arrays of square cylinders were investigated by Kim and Ghiaasiaan [17] and more recently by Pathak and Ghiaasiaan [18], with the objective of deriving solid-fluid interaction closure parameters that could be used in the standard unsteady volume-averaged momentum and energy conservation equation for flow in porous media. In [17] detailed numerical data for the porosity ranging from 0.64 to 0.84, with flow pulsation frequencies of 20–64 Hz were obtained. Based on these numerical data, the instantaneous as well as the cycle-average permeability and Forchheimer coefficients were derived. In [18], empirical correlations

Cryocoolers 17, edited by S.D. Miller and R.G. Ross, Jr.

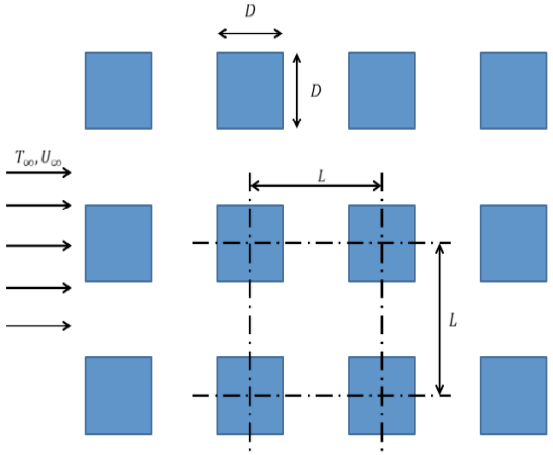

Figure 1. Physical configuration of parallel square rods in pulsating flow field comprising the porous medium of interest in this study.

for cycle-average pore-scale Nusselt number and the dimensionless thermal dispersion term were derived.

This study makes use of direct numerical simulation of flow in two-dimensional arrays of evenly spaced square rods to predict and analyze the viscous and thermal phenomena that occur when the rods are subjected to pulsating laminar flow. The objective is to examine the feasibility of using flow pulsations in order to enhance heat transfer in miniature heat exchangers.

SIMULATED SYSTEM

We consider tube bundles consisting of regularly spaced square rods arranged in a linear pattern with rows parallel to the direction of the pulsating flow field. The system modeled here is similar in design to the porous media previously investigated by Kim, Pathak, and Ghiaasiaan [17, 18] with modifications to improve solution clarity and to render the analysis relevant to heat exchangers. The modeled heat exchangers reported here consist of 10 rows of square cylinders as shown in Figure 1 (note that the figure shows only four rows) with unit fluid cells centered on the rods as shown in Figure 2.

The computational domain consists of 10 unit cells representing each of the 10 square blockages with edge length D and separated by length L, as well as buffer zones at the inlet and outlet of the array to ensure the velocity inlet boundary condition would be far enough from the

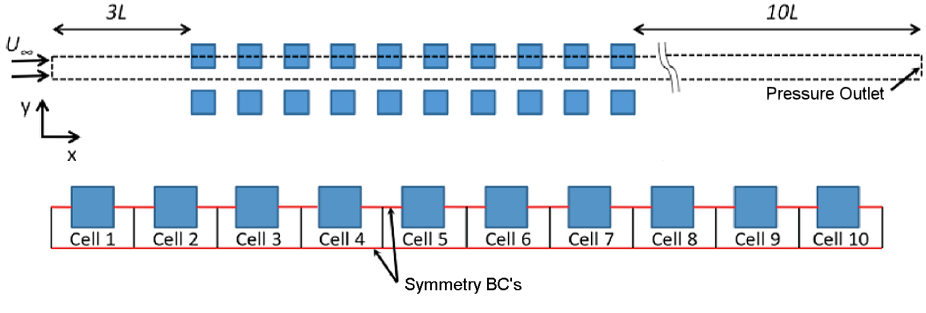

Figure 2. Computational domain for simulations indicated by dashed line. Symmetry conditions are indicated where used to improve computational efficiency.

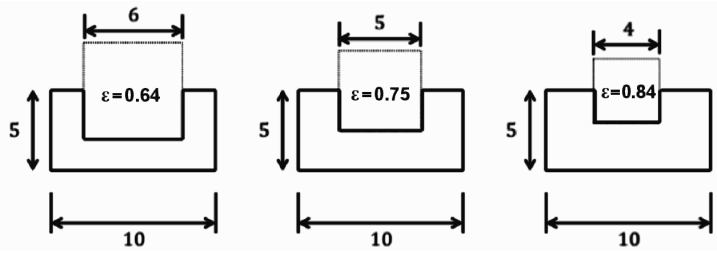

Figure 3. Unit cell configurations and dimensions (mm) for the porosities simulated. Dotted lines indicate the location of square tube blockage in relation to defined unit cell.

leading cell to ensure a negligible entrance effect. The outlet buffer was set to 10L to ensure the elimination of flow reversal at the pressure outlet boundary condition.

No-slip, isothermal wall boundary conditions were used to simulate the square rods. Meshing was performed in Gambit 2.4.6 [19] using 0.2 mm square elements, which has been shown to be more than sufficient to yield grid independence in previous studies with a similar simulated system [17]. Edge length D was parametrically adjusted while holding the spacing between cells L constant, in order to control the porosity ε, which will be discussed later. Three edge lengths are chosen as shown in Figure 3 to provide three separate porosities for simulation. More details can be found in [20].

THEORY AND SIMULATION

ANSYS® Fluent 13.0 [21] was used to numerically solve the mass, momentum and energy conservation equations for air as an incompressible Newtonian fluid. As mentioned previously, the square tubes are modeled here using no-slip, isothermal wall boundary conditions, where the heat flux through the walls is varied to maintain a constant surface temperature of 300 K.

Pulsating flow is defined as a sinusoidal oscillating flow superimposed on an otherwise steady flow at the inlet to the simulated system (location representing x=0 in Figure 1). The resulting net flow is therefore always positive in the x-direction (see Figure 1). The inlet velocity at x=0 is therefore found from:

$$U_\infty = U_m\left[1+0.25\sin\left(2\pi ft\right)\right] \tag{1}$$

The flow field is characterized in our simulations by the diameter-based Reynolds number defined based on the mean (time-average) inlet (superficial) velocity as:

$$\mathrm{Re}_D = \frac{\rho_f U_m D}{\mu_f} \tag{2}$$

Although little is known about the laminar-turbulent flow transition in porous media in unsteady flow, conditions leading to such transitions have been investigated in the past for steady flow. For this investigation the criterion suggested by Liu, *et al* [22] was used, whereby the maximum Reynolds number was limited to 250.

The drag coefficient, which represents the flow-induced forces on a rod, is an important parameter in view of the structural stability of heat exchangers:

$$C_D = \frac{2F_x}{\rho_f U_m^2} \tag{3}$$

The Nusselt number definition used herein is:

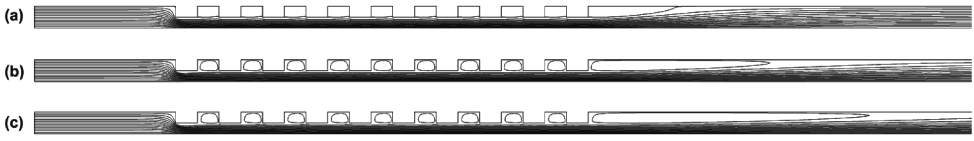

Figure 4. Typical steady flow stream functions for (a) Re_D=50 and (b) Re_D=125 and (c) Re_D=200.

$$Nu_D = \frac{hD}{k_f} = \frac{D}{k_f}\frac{\dot{Q}}{A\left(T_s - T_\infty\right)} \tag{1}$$

where $\dot{Q}$ is the total heat transfer rate from the solid surface in a unit cell, per unit depth. The heat transfer coefficient varies with time in pulsating flow; therefore the cycle-averaged quantity was employed.

Simulations were performed for Re_D=50, 125 and 200 such that, based on what is known about steady flow in porous media, with the peak velocity of $1.25U_m$, the flow would never transition into turbulent flow. Pulsation frequencies of 20-80 Hz were modeled, in addition to the steady-flow cases (representing zero frequency) performed for comparison. The pressure-based Navier-Stokes coupled solution algorithm of Fluent was used to solve the mass, continuity, and momentum conservation equations simultaneously. For all numerical simulations, the convergence criterion applied to the residuals for the continuity and momentum equations was a tolerance of 10^{-6}. A convergence criterion of 10^{-8} was used for the energy equation residuals.

RESULTS AND DISCUSSION

The overall characteristics of the flow fields being studied is displayed in Figure 4 for a typical steady flow simulation and in Figure 5 for a typical pulsating flow simulation. The latter figure shows seven snapshots of the pulsating flow field. In steady flow cases, behind each square blockage is a recirculation zone. Velocity vector plots of these recirculation zones from a similar system can be found in Kim and Ghiaasiaan [17] and are discussed in detail there.

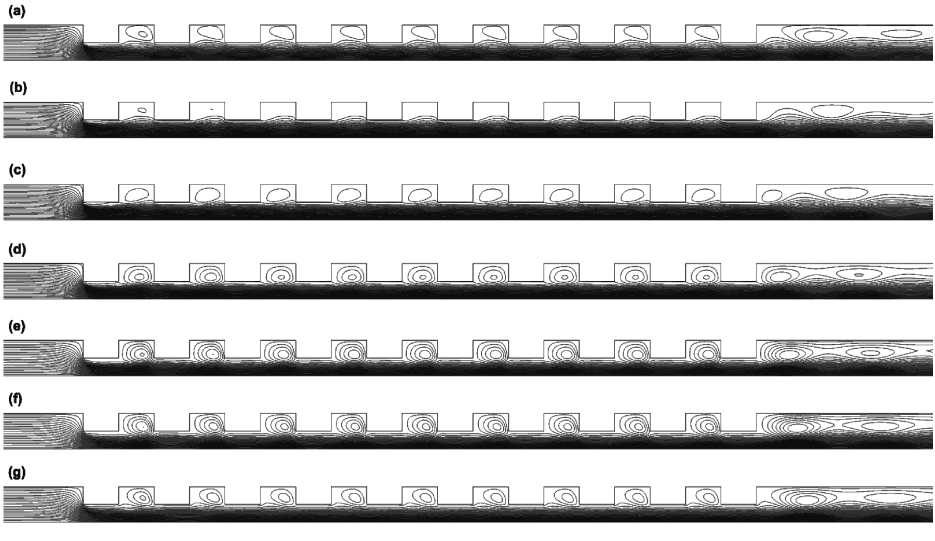

Figure 5. Pulsating flow stream functions at 7 evenly space points in a cycle for ε=0.75 Re_D=125 f=40 Hz. Defining $\theta=2\pi ft$: (a) θ=0°, (b) θ=60°, (c) θ=120°, (d) θ=180°, (e) θ=240°, (f) θ=300°, (g) θ=360°.

Drag

The drag force experienced by the leading tube was significantly larger than the drag on other rows. The trailing tubes not only experience smaller drag forces, but also in most cases their drag coefficient instantaneously reverses sign during each pulsation and becomes temporarily negative over a short period of time.

The resulting cycle-average drag coefficients are shown in Figure 6 and include some interesting trends. The cycle-average drag coefficient is always positive, as expected, despite the fact that the instantaneous coefficients can be negative for a portion of the cycle. The much larger magnitude of drag in the first tube compared to the trailing tubes is also apparent, and results from the wake interference effect. The variation in drag coefficient diminishes within the first 2-3 rows in all cases, with the following rows experiencing nearly the same drag forces. The plots also indicate that the cycle-average drag decreases almost exponentially with increasing Reynolds number, which is consistent with the trend for steady flow over single cylinders.

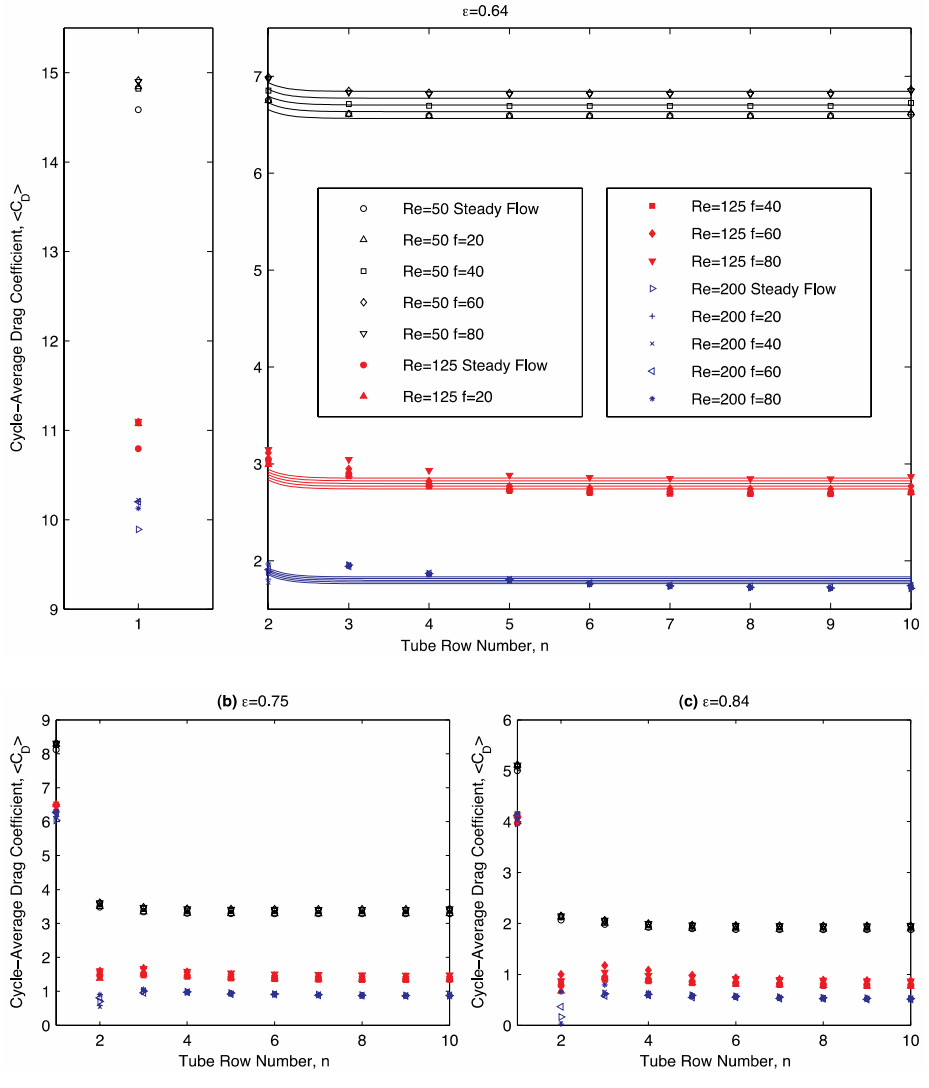

Figure 6. Cycle-average drag coefficients by tube number for various Re and frequencies (f in Hz).

The maximum drags coefficients, namely the peak drag coefficient during each cycle (not shown here for brevity) were also calculated. The maximum drag coefficient increased approximately linearly with frequency at the low Reynolds number, with the effect diminishing with increasing Reynolds number.

Heat transfer

The Nusselt number for the first row is significantly higher than other rows and the Nusselt number diminishes as the distance from the leading row is increased. This trend is of course consistent with the known trends in steady-flow heat transfer in exchanger tube bundles.

Most importantly, as noted in Figure 7, the flow pulsation enhances the fluid-tube heat transfer, and the level of enhancement increases monotonically with pulsation frequency. This is

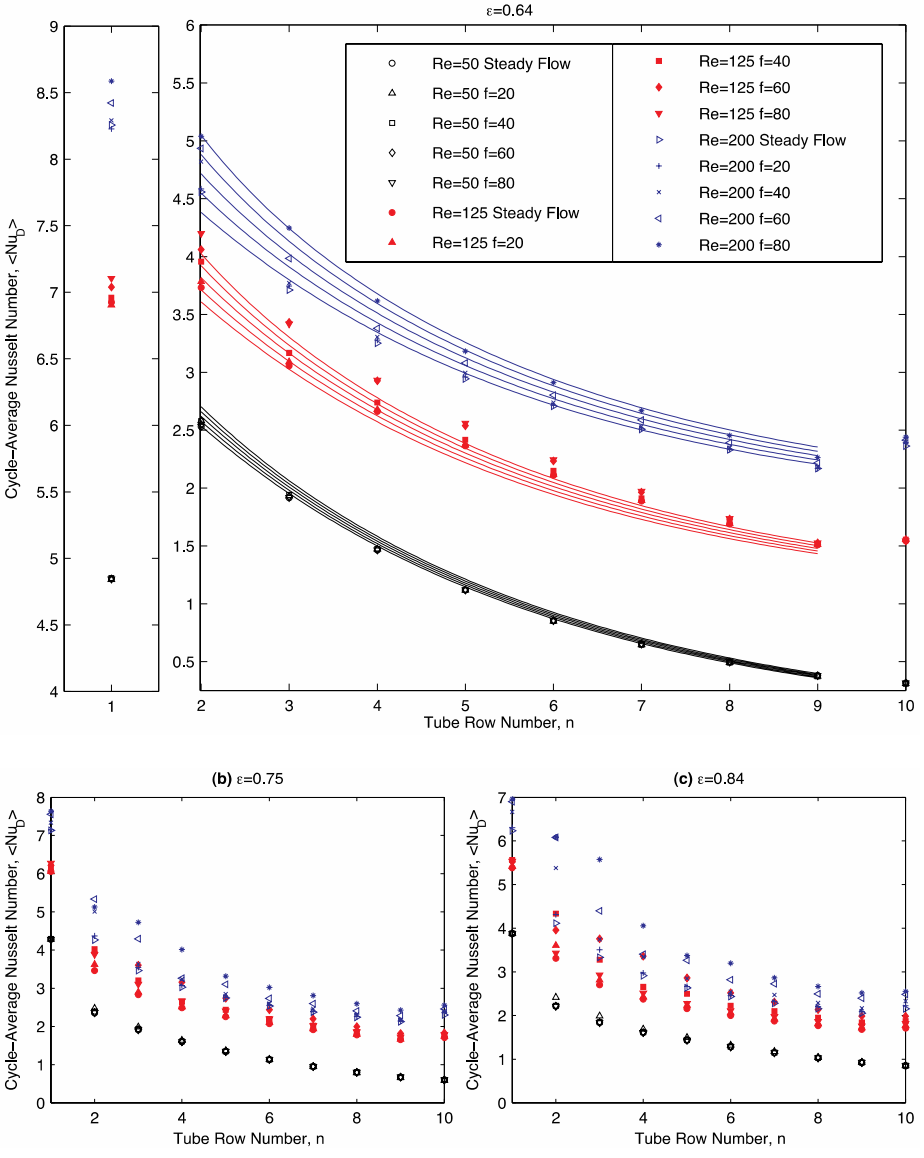

Figure 7. Cycle-average Nusselt number by tube number for various Re and frequencies (f in Hz).

consistent with Pathak and Ghiaasiaan [18], who also reported a monotonic increase in Nusselt number as a function of frequency in all cases they simulated, although the current study considers significantly lower Reynolds numbers. More information can be found in [20].

CONCLUDING REMARKS

Incompressible laminar pulsating flow through generic tube bundles composed of parallel square tubes configured in a square array was studied for porosities ranging from 64% to 84% over diameter-based Reynolds numbers in the range of 50-200. The effects of pulsation frequency were observed for frequencies in the 20 Hz – 80 Hz range, and were compared with steady flow cases. Cycle-average and maximum drag coefficients, and instantaneous and cycle-average Nusselt numbers were calculated and discussed. The cycle-average drag coefficient was observed to decrease with increasing porosity and Reynolds number, and was found to be insensitive to pulsation frequency, especially at high Reynolds numbers. The maximum drag coefficient increased approximately linearly with frequency at low Reynolds numbers, with the effect diminishing with increasing Reynolds number. The cycle-average Nusselt number was found to increase with both frequency and Reynolds number, with the frequency effect diminishing at very low Reynolds numbers.

The results of this study show that flow pulsations can enhance heat transfer in tube bundles, and the level of enhancement increases with pulsation frequency and mean flow Reynolds number.

REFERENCES

1. A. Zukauskas and R. Ulinskas, "Single-Phase Fluid Flow: Banks of Plain and Finned Tubes," *Heat Exchanger Design Handbook*, G. Hewitt, Ed., ed New York: Begell House, 1998.
2. A. Zukauskas, A. Skrinska, J. Ziugzda, and V. Gnielinski, "Single-Phase Convective Heat Transfer: Banks of Plain and Finned Tubes," *Heat Exchanger Design Handbook*, G. Hewitt, Ed., ed New York: Begell House, 1998.
3. V. Gnielinski, "Equations for Calculating Heat Transfer in Single Tube Rows and Banks of Tubes in Transverse Flow," *Int. Chem. Eng.,* vol. 19, pp. 380-391, 1979.
4. T. Nishimura, "Flow Across Tube Banks," *Encyclopedia of Fluid Mechanics*. vol. 1, N. P. Cheremisinoff, Ed., ed Houston: Gulf, 1986.
5. A.M.F. El-Shaboury and S. J. Ormiston, "Analysis of Laminar Forced Convection of Air Crossflow in In-line Tube Banks with Nonsquare Arrangement," *Num. Heat Transfer-A,* vol. 48, pp. 99-126, 2005.
6. K. Ishihara and K.J. Bell, "Friction Factors for In–line Square Tube Banks at Low Reynolds Numbers," *A.I. Ch.E Symp.,* vol. 68, pp. 74-80, 1972.
7. T. Nishimura and Y. Kawamura, "Analysis of Flow across Tube Banks in Low Reynolds Number Region," *J. Chem. Eng. Japan,* vol. 14, pp. 267-272, 1981.
8. C.K. Chen, K.L. Wong, and J.W. Cleaver, "Finite Element Solutions of Laminar Flow and Heat Transfer of Air in a Staggered and an In-Line Tube Bank," *Int. J. Heat Fluid Flow,* vol. 7, pp. 291-300, 1986.
9. K.L. Wong and C.K. Chen, "The Finite Element Solutions of Laminar Flow and Combined Convection of Air in a Staggered or an In-Line Tube-Bank," *Wärme- und Stoffübertragung,* vol. 23, pp. 93-101, 1988.
10. A.S. Wilson and M.K. Bassiouny, "Modeling of Heat Transfer for Flow across Tube Banks," *Chem. Eng. Proc.,* vol. 39, pp. 1-14, 2000.
11. M. Fujii, T. Fujii, and T. Nagata, "A Numerical Analysis of Laminar Flow and Heat Transfer of Air in an In-line Tube Bank," *Numer. Heat Transfer,* vol. 7, pp. 89-102, 1984.
12. M.N. Dhaubhadel, J.N. Reddy, and D.P. Telionis, "Penalty Finite-Element Analysis of Coupled Fluid Flow and Heat Transfer for In-Line Bundle of Cylinders in Cross Flow," *Int. J. Non–Linear Mech.,* vol. 21, pp. 361-373, 1986.

13. R. Radebaugh, "Development of the Pulse Tube Refrigerator as an Efficient and Reliable Cryocooler," *Proc. Institute of Refrigeration (London),* 1999.

14. J.S. Cha, *Hydrodynamic Parameters of Microporous Media for Steady and Oscillatory Flow: Application to Cryocooler Regenerator*, Doctoral Thesis, G.W. Woodruff School of Mechanical Engineering, Georgia Institute of Technology, 2007.

15. R.A. Ackerman, *Cryogenic Regenerative Heat Exchangers*. New York: Plenum Press, 1997.

16. J.S. Cha, S.M. Ghiaasiaan, and C.S. Kirkconnell, "Oscillatory flow in microporous media applied in pulse-tube and Stirling-cycle cryocooler regenerators," *Experimental Thermal and Fluid Science,* vol. 32, pp. 1264-1278, 2008.

17. S.-M. Kim and S.M. Ghiaasiaan, "Numerical modeling of laminar pulsating flow in porous media," *Journal of Fluids Engineering,* vol. 131, pp. 041203-1 - 041203-9, 2009.

18. M.G. Pathak and S.M. Ghiaasiaan, "Convective heat transfer and thermal dispersion during laminar pulsating flow in porous media," *International Journal of Thermal Sciences,* vol. 50, pp. 440-448, 2010.

19. *Gambit 2.4.6 User Guide*, ed: Fluent, Inc., 2006.

20. Mulacahey, T.I., Pathak, M.G., and Ghiaasiaan, S.M., " The effect of flow pulsation on drag and heat transfer in an array of heated square cylinders," *Int. J. Thermal Science*, to appear.

21. *ANSYS(R) Fluent, Release 13.0, help system, Fluent Theory Guide*, ed: ANSYS, Inc. , 2011.

22. S. Liu, A. Afacan, and J. Masliyah, "Steady incompressible laminar flow in porous media," *Chemical engineering science,* vol. 49, pp. 3565-3586, 1994.